Supporting Information

Hover et al. 10.1073/pnas.1500697112

SI Materials and Methods

General. Guanosine 5′-triphosphate (GTP), [U-^{13}C]GTP, SAM (as a toluenesulfonate salt), DTT, sodium dithionite, sulfanilamide, and 8-anilino-1-naphthalene sulfonic acid were purchased from Sigma-Aldrich. Δ*moaA*, Δ*moeB*, Δ*moaC E. coli* strains were obtained from the KEIO collection (1). Nonlinear least square fitting of kinetic data were carried out by using KaleidaGraph software (Synergy Software). Anaerobic experiments were carried out in an UNIlab workstation glove box (MBaun) maintained at 10 ± 2 °C with an O_2 concentration < 0.1 ppm. All HPLC experiments were performed on a Hitachi L-2130 Pump equipped with an L-2455 diode array detector, an L-2485 fluorescence detector, an L-2200 autosampler, and an ODS Hypersil C18 column (Thermo Scientific) housed in an L-2300 column oven maintained at 40 °C.

Expression and Purification of *Escherichia coli* MoaC. The untagged WT *E. coli* MoaC was homologously expressed in *E. coli* C41 (DE3) harboring a pMW15aC plasmid and purified by using a phenyl-Sepharose column (20 mL, HiTrap 16/10 Phenyl FF; GE), as described (2). For the expression of MoaC with a hexahistidine (His_6) tag at the N terminus, the pMW15aC plasmid was digested with NcoI and BamHI, and the *moaC* gene was subcloned into the corresponding site of pET30b (Novagen) to give pET-HisEcMoaC. The resulting plasmid was introduced into *E. coli* BL21(DE3), and His_6-tagged MoaC was expressed and purified as described (3). MoaC variants with mutations in one of the conserved amino acid residues (D17A, K21A, R26A, K51A, H77A, E112A, E114A, D128A, K131A, K147A) were prepared by following the Stratagene QuikChange site-directed mutagenesis protocol by using the primers shown in Table S2 and the pET-HisEcMoaC or pMW15aC plasmid as a template.

In situ ^{13}C NMR Characterization of MoaA Products. The MoaA assay was performed under strict anaerobic conditions in the presence of MoaA (0.4 mM), SAM (1 mM), [U-^{13}C]GTP (1 mM), sodium dithionite (5 mM) in the assay buffer (50 mM Tris·HCl pH 7.6, 1 mM $MgCl_2$, 2 mM DTT, and 0.3 M NaCl) at 25 °C for 120 min. After incubation, a final volume of 5% (vol/vol) anaerobic D_2O was added and the resulting solution was transferred to an NMR tube, sealed under anaerobic conditions (O_2 < 0.1 ppm) and immediately subjected to ^{13}C NMR analysis. The ^{13}C NMR data were collected at 6 °C for 16 h. No apparent change in the spectra was observed before and after the data collection. The ^{13}C NMR spectrum of [U-^{13}C]3′,8-cH$_2$GTP was determined by using the molecule purified as described (3).

HPLC and LC-MS Characterization of MoaA Products. To chemically characterize MoaA products, purified WT-MoaA (65 μM) was anaerobically incubated with GTP (0.2 mM), SAM (1 mM), and sodium dithionite (1 mM) in the assay buffer (50 mM Tris·HCl pH 7.6, 1 mM $MgCl_2$, 2 mM DTT, and 0.3 M NaCl) at 25 °C. After incubation for 5, 20, 80, or 240 min, 30 μL of the reaction sample was removed, and added to 20 μL of assay buffer with or without WT-MoaC (545 μM). After additional incubation for 5 min at 25 °C, 3 μL of anaerobic assay buffer containing 310 μM calf intestinal phosphatase (CIP; NEB MO29OS) was added and incubated for 60 min at 25 °C. The resulting solution was subsequently mixed with 0.1 volume of an anaerobic solution of I_2 [5% (wt/vol)] and KI [10% (wt/vol)], and incubated for 60 min at 22 °C. The resulting mixture was analyzed by HPLC equipped with an ODS Hypersil C18 column (4.6 × 150 mm, 3 μm; Thermo Scientific part 30103-154630). The elution was performed by a linear gradient at 1.2 mL/min by using 30 mM ammonium formate, pH 4.5 (solvent A) and 100% MeOH (solvent B): 0–15% B for 12 min, and monitored by fluorescence [excitation (Ex.) 365 nm, emission (Em.) 445 nm]. Under this condition, compound Z (the fluorescent derivative of cPMP) was eluted at 2.0 min, and the fluorescent derivative of the minor MoaA product was eluted at 2.9 min. The amount of compound Z was quantified as described (3).

For LC-MS analysis, the assay was performed by using WT-MoaA (250 μM), GTP (0.5 mM), SAM (0.5 mM), and sodium dithionite (2 mM) in the assay buffer at 25 °C for 300 min. The resulting solution was treated with CIP and then KI/I_2 without incubation with MoaC. The fluorescent derivative was HPLC purified (the peak at 2.9 min retention time), lyophilized, and then analyzed in positive ion mode by using an Agilent LC-ESI-TOF-MS equipped with an Agilent Poroshell 120 C18 column (2.1 × 75 mm, 2.7 μm; part 697775-906). The elution was performed by a linear gradient at 0.7 mL/min by using 0.3% formic acid, pH 2.0 (solvent A) and 100% acetonitile (solvent B): 2–85% B for 20 min. Data were analyzed by using Agilent Masshunter software.

In Vitro Characterization of MoaC. For the coupled assay, purified WT or a variant of MoaC (0.5 μM) was anaerobically incubated with MoaA (1 μM), GTP (1 mM), SAM (1 mM), and sodium dithionite (1 mM) in the assay buffer at 25 °C for 60 min. The reaction was then quenched with 0.1 volume of 25% (wt/vol) trichloroacetic acid (TCA), and cPMP was quantified by HPLC after its conversion to compound Z (3). For the steady-state kinetic analysis, 3′,8-cH$_2$GTP was isolated from the in vitro assay solution of MoaA as reported under strict anaerobic conditions (<0.1 ppm O_2) (3). Based on NMR and HPLC, the purity of 3′,8-cH$_2$GTP used in this study was greater than 95%. MoaC (0.1 or 1 μM) was anaerobically incubated with purified 3′,8-cH$_2$GTP at specified concentrations (Fig. S3) in assay buffer at 25 °C. The reaction was initiated by the addition of MoaC, and an aliquot (90 μL) was removed at each time point and mixed with 10 μL of 25% (wt/vol) TCA to stop the reaction. cPMP was quantified by HPLC, as described above.

In Vivo Characterization of MoaC. For the complementation of *E. coli* Δ*moaC* with MoaC variants, the pET-HisEcMoaC plasmid was digested with XbaI and HindIII, and the *moaC* gene (WT or a variant) was subcloned into the corresponding site of pBAD33 (ATCC) to give pBAD33-HisEcMoaC. To test the activity of MoaC variants in vivo, the pBAD33-HisEcMoaC plasmid harboring one of the MoaC variants was introduced into the *E. coli* Δ*moaC* strain. The resulting transformants (*E. coli* Δ*moaC*/pBAD33-HisEcMoaC) were cultured for 16 h at 37 °C in LB media supplemented with kanamycin (50 mg/L) and chloramphenicol (34 mg/L). The cells from a 0.5-mL aliquot of these overnight cultures were pelleted and the media was removed. Cell pellets were brought inside an anaerobic glove box (<1 ppm O_2) and resuspended in 15 mL of anaerobic PN medium (4) supplemented with $NaNO_3$ (100 mM), kanamycin (50 mg/L), chloramphenicol (34 mg/L), 0.4% (wt/vol) glucose, and 1× trace metals (5). Cultures were grown over 24 h at 22 °C while shaking and the OD_{600} was monitored. To determine the NR activity, the cells were harvested after 24 h by centrifugation (5,000 × *g*, 20 min, 4 °C), resuspended in 1 mL of 250 mM NaH_2PO_4 pH 7.1, and lysed at 4 °C by sonication using a Branson Digital Sonifier at 30% amplitude for 30 s with 0.5-s pulses. The protein concentration

of the cell lysate was determined by the Bradford assay (Amresco). NR assays were performed at 22 °C by using the whole-cell lysate (100 μg/mL), 52.4 mM $NaNO_3$, 1.3 mM DTT, 0.204 μM methyl viologen, 2.2 μM sodium dithionite in 250 mM NaH_2PO_4 pH 7.1 (500 μL). The reaction was quenched by vigorous mixing with air, and nitrite was quantified by the diazocoupling derivatization method (6).

Western Blot. Basal expression levels of His_6-MoaC from the uninduced pBAD33-HisEcMoaC–complemented Δ*moaC E. coli* growths were assessed by Western blotting. SDS/PAGE was performed under reducing conditions on whole-cell lysate by using 12.5% (wt/vol) polyacrylamide gels with 1–10 μg of total cellular protein per lane. After electrophoresis, proteins were transferred to a nitrocellulose membrane at 2.5 A for 20 min. His_6-MoaC was detected by using anti-polyhistidine tag mAbs (Thermo Scientific) and peroxidase-coupled anti-mouse Ig (Southern Biotech). The observed bands were quantified based on comparison with bands of purified His_6-MoaC standards (0, 0.34, 1.0, 3.1 pmol per lane). The concentrations of MoaC in *E. coli* cells were calculated based on cell counting (1×10^9 cells per mL/OD_{600}), and the reported volume of an *E. coli* cell as 0.85 fL (7).

Crystallography and Structure Determination. *E. coli* MoaC was crystallized by hanging drop vapor diffusion using a 1:1 ratio of 10 mg/mL MoaC to 35% (wt/vol) PEG 1500 and 0.1 M MMT buffer [1:2:2 DL-Malic acid:Mes(*N*-morpholino)ethane-sulfonic acid] at pH 9.0. Hexagonal bipyramidal crystals grew after 4 d at 22 °C. For soaking experiments, the apo crystals were transferred to a 3-μL drop of the crystallization solution on a coverslip in an anaerobic environment (<0.1 ppm O_2) at 10 °C, and left to exchange for 1 h with either 3′,8-cH_2GTP or cPMP at final concentrations of 0.27 mM and 0.83 mM, respectively. The coverslip was then sealed over an empty well for 15 h, which led to partial dehydration of the crystals and improved diffraction. For data collection, the crystals were cryopreserved by using the crystallization solution supplemented with 22% (vol/vol) ethylene glycol. X-ray intensity data were collected on a R-AXIS HTC imaging plate area detector mounted on a Rigaku FRE+ SuperBright rotating anode generator by using Cu Kα radiation, or at the South Eastern Regional Collaborative Access Team 22-ID line at the Advanced Photon Source (Argonne National Laboratory). The data were processed with HKL3000 (8). All crystals took the hexagonal space group $P6_322$ except the cPMP-soaked crystals in which soaking resulted in an alteration of the symmetry to the orthorhombic space group $P2_12_12_1$. The structures were solved by molecular replacement using the apo *E. coli* MoaC structure as a search model (PDB ID code: 1EKR) with PHASER (9). Subsequent model building was carried out by using COOT, (10) and refinement was performed in PHENIX (11). Confirmation of a bound ligand was determined by dissolving cocrystals after data collection and analyzing by HPLC for 3′,8-cH_2GTP or cPMP as described (3). Coordinates and structure factors for the K51A-MoaC•3′,8-cH_2GTP, and WT-MoaC•cPMP structures have been deposited in the Protein Data Bank under the ID codes 4PYA and 4PYD, respectively.

Anaerobic HPLC and LCMS Analysis of the Products of MoaC Variants. MoaC assays were performed at 25 °C under anaerobic conditions (O_2 <0.1 ppm) by using either 3′,8-cH_2GTP or Intermediate X as substrates. In these assays, 3′,8-cH_2GTP was generated in situ by incubating MoaA (40 μM) with SAM (1 mM), GTP (1 mM), and sodium dithionite (1 mM) in the assay buffer at 25 °C. After 120 min, where no further turnover is detectable (Fig. 2*D*), WT or variant of MoaC was added to the final concentration of 120 μM and the reaction was incubated for another 120 min. For the reaction of Intermediate X with WT-MoaC, the products from the K131A-MoaC assay was filtered with a 10-kDa molecular weight cutoff (MWCO) filter after 120 min, where >90% of 3′,8-cH_2GTP is converted to Intermediate X, and combined with a final concentration of 25 μM WT-MoaC for 1 h at 25 °C under anaerobic conditions. All reactions were subsequently quenched by addition of stoichiometric volume of anaerobic MeOH, and the protein precipitant was removed. An aliquot of supernatant (60 μL) was analyzed by anaerobic HPLC using an Alltech Apollo C18 4.6 × 250 mm, 2.7-μm column (part 36511) equilibrated in anaerobic 0.1 M KH_2PO_4, pH 6.0, 8 mM tetrabutylammonium hydrogen sulfate (Solvent A). The elution was made with a flow rate at 1.0 mL/min by using solvent A and solvent B [0.1 M KH_2PO_4, pH 6.0, 8 mM tetrabutylammonium hydrogen sulfate, 30% (vol/vol) ACN]: 0% B for 6.5 min, 0–20% B for 6.5 min, 20–40% B for 13 min, 40–100% B for 8 min. Chromatography was monitored by diode array detector.

For LC-MS analysis, the enzyme activity assays were setup as described above, but in 50 mM ammonium bicarbonate, pH 8.0, instead of the assay buffer. After the incubation with MoaC for 120 min, the solutions were combined with 3 μL of anaerobic CIP (310 μM), incubated for 60 min at 25 °C, and filtered with a 10-kDa MWCO filter. A portion of the filtrate (10 μL) were analyzed anaerobically in positive ion-mode by using an Agilent LC-ESI-TOF-MS equipped with an Agilent Poroshell 120 C18 column (2.1 × 75 mm, 2.7 μm, part 697775-906). The elution was made with a flow rate at 0.15 mL/min by using anaerobic 30 mM ammonium acetate, pH 8.0 (solvent A) and 100% MeOH (solvent B): 0–2% B for 10 min, 2–50% B for 7 min, 50–100% B for 5 min. Data were analyzed by using Agilent Masshunter software.

Chemical Characterization of Intermediate X. For chemical characterization, Intermediate X and 3′,8-cH_2GTP was generated as described above for the anaerobic HPLC characterization, except that 65 μM MoaA was used. The reactions were derivatized to either DMPT or compound Z and analyzed by HPLC as described (3).

1. Baba T, et al. (2006) Construction of Escherichia coli K-12 in-frame, single-gene knockout mutants: The Keio collection. *Mol Syst Biol* 2:2006.0008.
2. Wuebbens MM, Liu MT, Rajagopalan K, Schindelin H (2000) Insights into molybdenum cofactor deficiency provided by the crystal structure of the molybdenum cofactor biosynthesis protein MoaC. *Structure* 8(7):709–718.
3. Hover BM, Loksztejn A, Ribeiro AA, Yokoyama K (2013) Identification of a cyclic nucleotide as a cryptic intermediate in molybdenum cofactor biosynthesis. *J Am Chem Soc* 135(18):7019–7032.
4. Stewart V, MacGregor CH (1982) Nitrate reductase in Escherichia coli K-12: Involvement of chlC, chlE, and chlG loci. *J Bacteriol* 151(2):788–799.
5. Studier FW (2005) Protein production by auto-induction in high density shaking cultures. *Protein Expr Purif* 41(1):207–234.
6. MacGregor CH, Schnaitman CA, Normansell DE (1974) Purification and properties of nitrate reductase from Escherichia coli K12. *J Biol Chem* 249(16):5321–5327.
7. Neidhardt FC, Ingraham JL (1987) *Escherichia coli and Salmonella typhimurium: Cellular and Molecular Biology* (Am Soc Microbiol, Washington).
8. Minor W, Cymborowski M, Otwinowski Z, Chruszcz M (2006) HKL-3000: The integration of data reduction and structure solution—from diffraction images to an initial model in minutes. *Acta Crystallogr D Biol Crystallogr* 62(Pt 8):859–866.
9. Bunkóczi G, et al. (2013) Phaser.MRage: Automated molecular replacement. *Acta Crystallogr D Biol Crystallogr* 69(Pt 11):2276–2286.
10. Emsley P, Lohkamp B, Scott WG, Cowtan K (2010) Features and development of Coot. *Acta Crystallogr D Biol Crystallogr* 66(Pt 4):486–501.
11. Adams PD, et al. (2010) PHENIX: A comprehensive Python-based system for macromolecular structure solution. *Acta Crystallogr D Biol Crystallogr* 66(Pt 2):213–221.

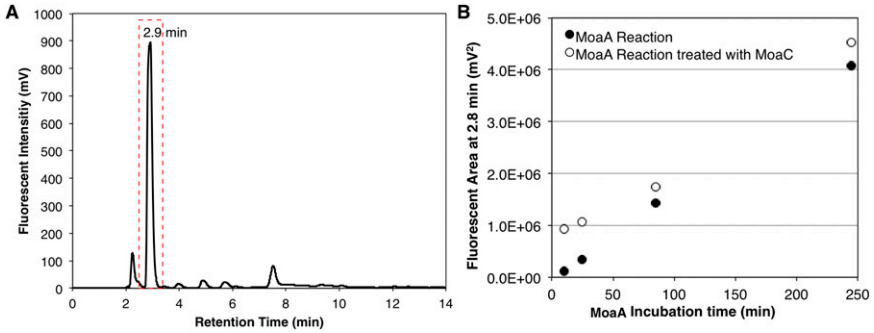

Fig. S1. Detection and characterization of minor MoaA products. (*A*) HPLC analysis of MoaA products after KI/I_2 treatment. MoaA reaction products were treated with calf intestine phosphatase (CIP), followed by KI/I_2 at pH 7.5 under strict anaerobic conditions as reported (1). The resulting products were analyzed by an HPLC equipped with an ODS Hypersil C18 column, and the elution monitored by fluorescence (Ex. 365 nm, Em. 450 nm). No fluorescent peaks related to the MoaA reaction was observed outside the shown chromatography range. The formation of the peak at 2.9 min (highlighted in a red dashed square) depended on MoaA. (*B*) Time course of the formation of the peak in *A* at the 2.9 min retention time, with and without MoaC treatment (open and filled circles, respectively). The MoaA assay was performed in the absence of MoaC for the specified incubation time, followed by an addition of assay buffer with or without MoaC. After additional incubation for 5 min, products were then derivatized as described in *A*. No decrease of the fluorescent derivative was observed upon MoaC incubation, suggesting that the observed molecule does not serve as the MoaC substrate. Based on comparisons with related pterin compounds (compound Z and dimethylpterin), the amount of the fluorescent molecule was estimated as ~0.2, 0.4, 2, and 4 μM at 10, 25, 85, and 245 min, respectively. Based on this estimation, the rate of formation of this compound is $\sim 2.6 \times 10^{-4}$ min^{-1}, which is 200-fold slower than that of 3′,8-cH_2GTP formation (0.05 min^{-1}).

1. Mehta AP, Abdelwahed SH, Xu H, Begley TP (2014) Molybdopterin biosynthesis: Trapping of intermediates for theMoaA-catalyzed reaction using 2′-deoxyGTP and 2′-chloroGTP as substrate analogues. *J Am Chem Soc* 136(30):10609–10614.

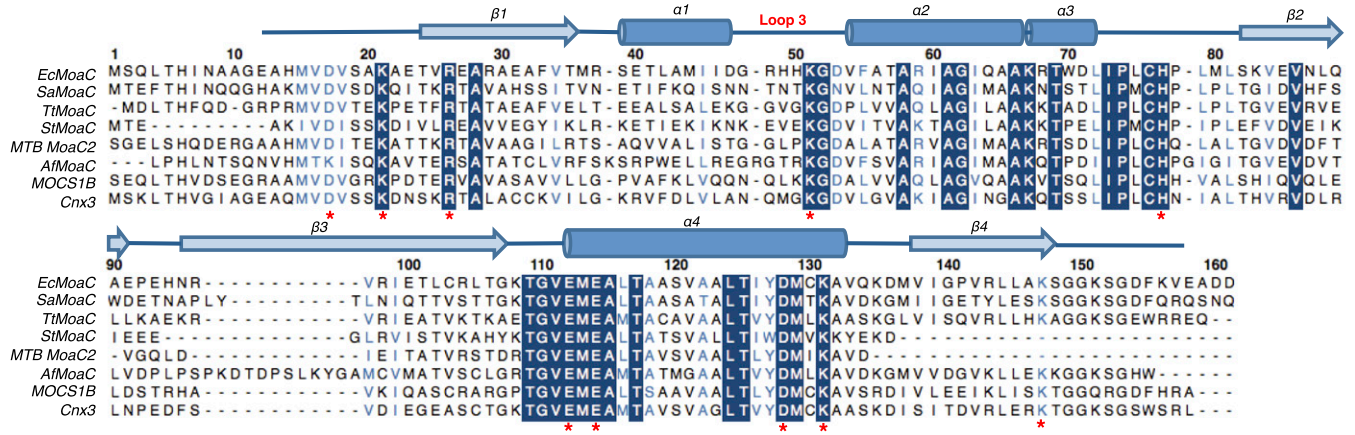

Fig. S2. Amino acid sequence alignment of MoaC. *E. coli* MoaC, *Staphylococcus aureus* MoaC, *Thermus thermophilus* MoaC, *Sulfolobus tokodaii* MoaC, *Mycobacterium tuberculosis* MoaC2, *Aspergillus fumigatus* MoaC, *Homo sapiens* MOCS1B, and *Arabidopsis* thaliana Cnx3. Conserved residues are highlighted in blue. The residues investigated in this study are indicated by red asterisks.

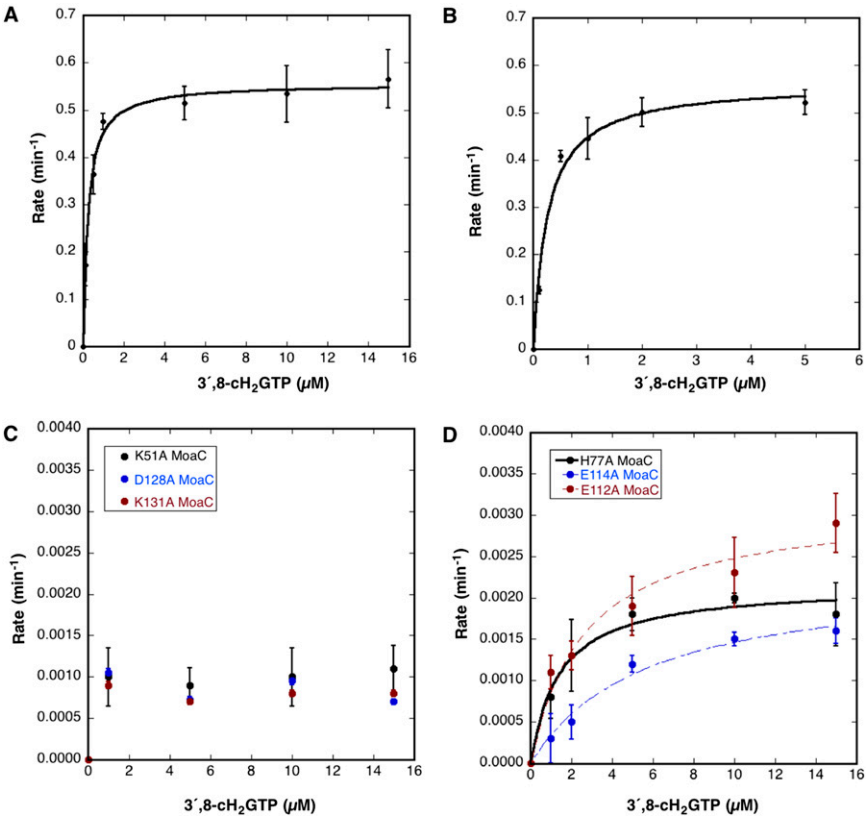

Fig. S3. Steady-state kinetic characterization of WT and variants of MoaC. The rates of the conversion of 3′,8-cH$_2$GTP into cPMP were determined by using WT His$_6$-MoaC (0.1 μM) and 3′,8-cH$_2$GTP (0, 0.1, 0.5, 1.0, 5.0, 10, 15 μM) (*A*); WT-MoaC (nontagged, 0.1 μM) and 3′,8-cH$_2$GTP (0, 0.1, 0.5, 1.0, 2.0, 5.0 μM) (*B*); K51A, D128A, or K131A MoaC (1.0 μM) and 3′,8-cH$_2$GTP (0, 1.0, 5.0, 10, 15 μM) (*C*); an H77A, E112A, or E114A MoaC (1.0 μM) and 3′,8-cH$_2$GTP (0, 1.0, 2.0, 5.0, 10, 15 μM) (*D*). Solid lines are nonlinear fits to the Michaelis–Menten equation with k_{cat} and K_m values provided in Fig. 1*F*. In *C*, the catalytic rates for K51A, D128A, and K131A MoaC were not affected by the tested range of substrate concentrations (1–15 μM), presumably because of the low K_m values (<1.0 μM; compare data in *A* and *B*). Kinetic measurements below 1.0 μM 3′,8-cH$_2$GTP were not possible because of the limit of detection for cPMP, and the slow rate of catalysis by these MoaC variants. Therefore, the k_{cat} values for these variants (Fig. 1*F*) were deduced from the averages of the observed catalytic rate and only the upper limits for the K_m values were reported. All data are averages of two or three replicates, and error bars are the SDs among the replicates.

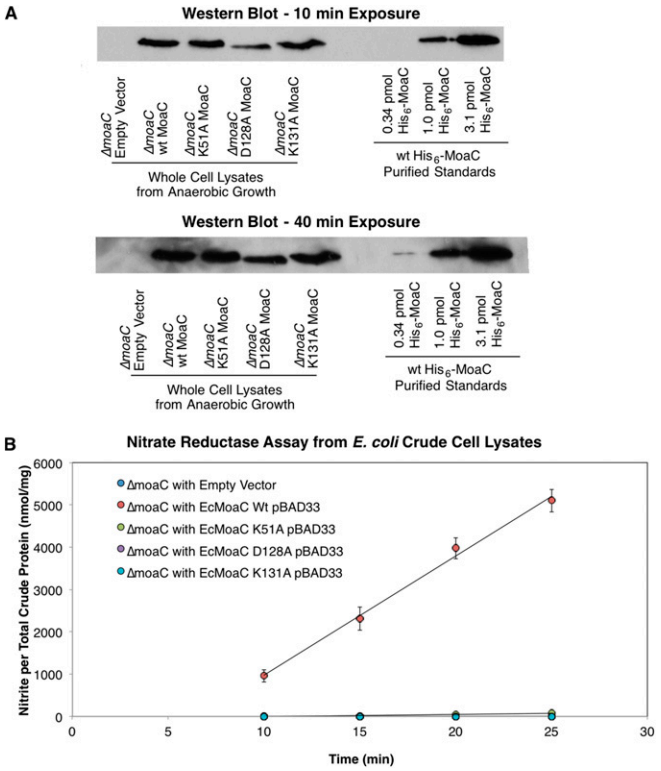

Fig. S4. In vivo assay of MoaC variants. (*A*) Western blot detection of His_6-MoaC expressed in *E. coli* Δ*moaC*. The concentrations of MoaC inside the cells are estimated as 7.9, 7.7, 4.5, and 7.6 nM for Δ*moaC*/WT-MoaC, Δ*moaC*/D51A-MoaC, Δ*moaC*/D128A-MoaC, and Δ*moaC*/K131A-MoaC, respectively. (*B*) Timecourse of the nitrate reductase assay.

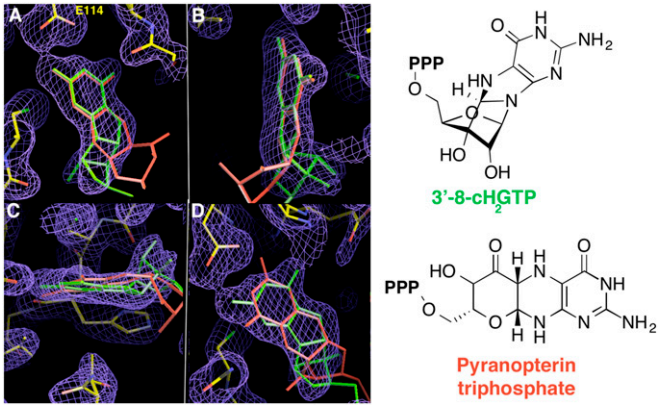

Fig. S5. Analysis of electron density observed in the putative MoaC active site. The omit map (purple mesh) was calculated after 50 rounds of refinement without any ligand to minimize model-derived bias and then fit to 3′,8-cH_2GTP (green) or pyranopterin triphosphate (red). MoaC amino acid side chains are shown as yellow sticks. (*A*–*C*) Fitting attempts started by using the common aminopyrimidinone moiety (which is tightly anchored by specific H bonds from the E114 side chain to the guanine N1 and N2 atoms) as an anchor point. An optimal fit was achieved with 3′,8-cH_2GTP for the entire molecule. However, the electron density does not accommodate the third ring of the pyranopterin triphosphate. (*D*) An attempt to fit the third ring of the pyranopterin triphosphate model (red) still failed to provide optimal overlap with the density curvature. Moreover, this fit requires that the aminopyrimidinone moiety is flipped, which removes the guanine moiety from the density. Additionally, in this position, the H-bonding interaction between E114 and the N1 atom of the aminopyrimidinone ring is abrogated, and the O6 atom clashes with the E114 side chain Oε1. The fit to 3′,8-cH_2GTP (green) is identical to those shown in *A*–*C*.

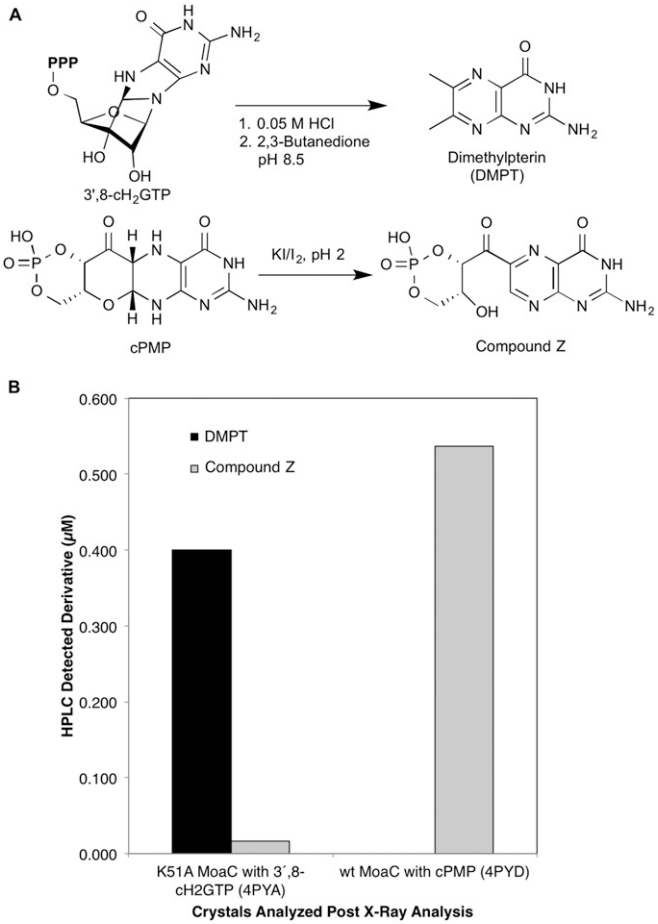

Fig. S6. HPLC analyses of 3′,8-cH$_2$GTP and cPMP in MoaC crystals. (*A*) Derivatization scheme for 3′,8-cH$_2$GTP and cPMP to dimethylpterin (DMPT) and compound Z, respectively (3). (*B*) HPLC quantitation of 3′,8-cH$_2$GTP and cPMP in MoaC crystals used for structure determination. Crystals were dissolved in 2.5% (wt/vol) TCA after data collection to prevent any potential catalytic turnover. Then, 3′,8-cH$_2$GTP and cPMP were derivatized to dimethylpterin (DMPT) or compound Z, respectively, and quantified by HPLC as described in *Methods*. The presence of 3′,8-cH$_2$GTP in the crystals of K51A-MoaC, and the presence of cPMP in WT-MoaC were consistent with the electron density observed within the active-site pocket.

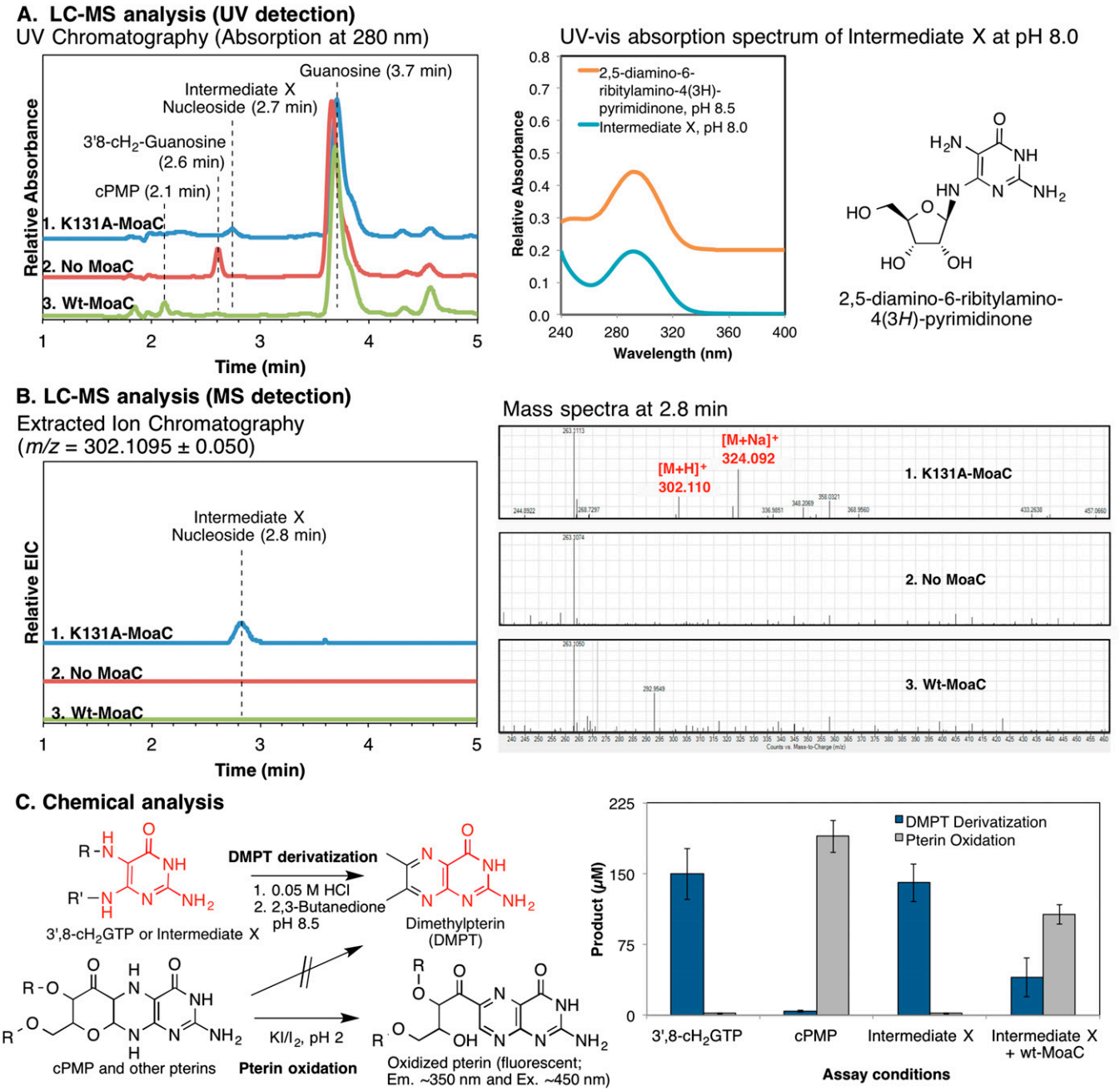

Fig. S7. Characterization of Intermediate X. (*A* and *B*) LC-MS analysis of WT or K131A-MoaC assay products. Shown are the UV (*A*, 280 nm) and extracted ion (*B*, *m/z* = 302.1095 ± 0.050) chromatography of products from the reactions with K131A-MoaC (trace 1), without MoaC (trace 2), and with WT-MoaC (trace 3). In all assays, 3′,8-cH$_2$GTP was used as the substrate, and the products were treated with CIP before the analyses. The elution time difference between UV and ESI-TOF mass detection was ~0.1 min. Shown in *A, Right* is a UV-absorption spectrum of Intermediate X nucleoside (blue trace) determined by the diode array detection of the LC elution at 2.7 min in trace 1, compared with reported spectrum of 2,5-diamino-6-ribitylamino-4(3*H*)-pyrimidinone at pH 8.5 (1) (yellow trace). At pH 8.0, Intermediate X exhibits only the absorption band at λ_{max} = 290 nm, whereas at pH 6.5 (Fig. 4*B*) Intermediate X absorbs at both λ_{max} = 272 and 290 nm. Based on the reported pK_a values of triaminopyrimidinone containing molecules (2, 3), we attributed the difference to the change in the protonation states at pH 6.5 and 8.0. Shown in *B*, *Right* are the mass spectra at retention time of 2.8 min. The signals unique to the K131A-MoaC reaction were highlighted in red bold. (*C*) Chemical characterization of Intermediate X. Top half of the scheme describes DMPT derivatization for the detection of molecules with acid-labile triaminopyrimidinone base (highlighted in red). Examples of such molecules include 3′,8-cH$_2$GTP and 2,5-diamino-6-ribitylamino-4(3*H*)-pyrimidinone (see the structure in *A*). Pyranopterin and other pterin molecules are not converted to DMPT under these conditions, but can be oxidized to a fluorescent pterin by KI/I$_2$ treatment (pterin oxidation, bottom). Shown in *C, Right* are the results of the chemical derivatization of 3′,8-cH$_2$GTP, cPMP, Intermediate X, and Intermediate X incubated with WT-MoaC. As reported previously (4), 3′,8-cH$_2$GTP and cPMP were derivatized to DMPT and oxidized pterin, respectively. Intermediate X was converted to DMPT, but not to the oxidized pterin, suggesting that Intermediate X harbors an acid labile triaminopyrimidinone base, but not the pterin structure. However, when Intermediate X was incubated with WT-MoaC, the resulting molecule was converted to the oxidized pterin, consistent with the formation of cPMP. DMPT detected in this sample is derived from residual Intermediate X, which is consistent with the anaerobic HPLC analysis (Fig. 4*A*, trace 9). All of these observations suggest that Intermediate X has an acid labile triaminopyrimidinone base and is converted to cPMP upon incubation with WT-MoaC.

1. Schramek N, et al. (2002) Reaction mechanism of GTP cyclohydrolase I: Single turnover experiments using a kinetically competent reaction intermediate. *J Mol Biol* 316(3):829–837.
2. Goyal RN, Kumar A, Jain N, Gupta P (1999) Electrochemical oxidation of 6-hydroxy-2,4,5triaminopyrimidine at pyrolytic graphite electrode. *Indian J Chem A* 38(10):1015–1023.
3. Pohland A, Flynn EH, Jones RG, Shive W (1951) A proposed structure for folinic acid-SF, a growth factor derived from pteroylglutamic acid. *J Am Chem Soc* 73(7):3247–3252.
4. Emsley P, Lohkamp B, Scott WG, Cowtan K (2010) Features and development of Coot. *Acta Crystallogr D Biol Crystallogr* 66(Pt 4):486–501.

Table S1. Data collection and refinement statistics

	MoaC-K51A•3′,8-cH$_2$GTP (4PYA)	MoaC-cPMP (4PYD)
Data collection		
Space group	$P6_322$	$P2_12_12_1$
Cell dimensions		
a, *b*, *c*, Å	89.93, 89.93, 62.45	61.59, 97.21, 165.33
α, β, γ, °	90, 90, 120	90, 90, 90
Resolution, Å	29–1.79 (1.85–1.79)*	38–3.18 (3.23–3.18)
R_{sym}, %	5.8 (67.5)	10.2 (64.7)
$I/\sigma I$	50.7 (2.2)	18.6 (2.4)
Completeness, %	99.6 (99.6)	99.9 (100)
Redundancy	6.8 (5.6)	7.0 (6.9)
Refinement		
Resolution, Å	1.78	3.18
No. of reflections	14,509	17,076
R_{work}/R_{free}, %	17.4/19.4	23.2/29.6
No. of atoms	1064	6498
Macromolecule	949	6378
3′,8-cH$_2$GTP or cPMP	32	23
Solvent	55	0
B factors, Å^2	47.4	68.6
Macromolecule	45.5	68.6
3′,8-cH$_2$GTP or cPMP	82.1	68.7
Solvent	49.5	—
R.m.s. deviations		
Bond lengths, Å	0.009	0.009
Bond angles, °	1.408	1.290
Ramachandran analysis		
Ramachandran favored, %	98.0	98.5
Ramachandran outliers, %	0	0

*Values in parentheses are for highest-resolution shell.

Table S2. PCR primers used in this study

Primers	Sequence
D17A-f	5′-CGCACATGGTGGCGGTCTCCGCCAAAG-3′
D17A-r	5′-CTTTGGCGGAGACCGCCACCATGTGCG-3′
K21A-f	5′-TGGATGTCTCCGCCGCGGCGGAAACCGTGCGT-3′
K21A-r	5′-ACGCACGGTTTCCGCCGCGGCGGAGACATCCA-3′
R26A-f	5′-CAAAGCGGAAACCGTGGCGGAAGCGCGGGCGGAAG-3′
R26A-r	5′-CTTCCGCCCGCGCTTCCGCCACGGTTTCCGCTTTG-3′
K51A-f	5′-GATGGTCGCCACCACGCGGGCGACGTATTTGC-3′
K51A-r	5′-GCAAATACGTCGCCCGCGTGGTGGCGACCATC-3′
H77A-f	5′-CCCGCTCTGTGCTCCGCTGATGC-3′
H77A-r	5′-GCATCAGCGGAGCACAGAGCGGG-3′
G110R-f	5′-CTGACCGGGAAAACCCGTGTCGAAATGGAAG-3′
G110R-r	5′-CTTCCATTTCGACACGGGTTTTCCCGGTCAG-3′
E112A-f	5′-GAAAACCGGTGTCGCGATGGAAGCATTAAC-3′
E112A-r	5′-GTTAATGCTTCCATCGCGACACCGGTTTTC-3′
E114A-f	5′-GTGTCGAAATGGCGGCATTAACCGC-3′
E114A-r	5′-GCGGTTAATGCCGCCATTTCGACAC-3′
T117P-f	5′-GAAATGGAAGCATTACCGGCGGCCTCCGTG-3′
T117P-r	5′-CACGGAGGCCGCCGGTAATGCTTCCATTTC-3′
D128A-f	5′-GCGCTGACCATTTATGCGATGTGCAAAGCGGTG-3′
D128A-r	5′-CACCGCTTTGCACATCGCATAAATGGTCAGCGC-3′
K131A-f	5′-CCATTTATGACATGTGCGCGGCGGTGCAAAAAGATATG-3′
K131A-r	5′-CATATCTTTTTGCACCGCCGCGCACATGTCATAAATGG-3′
K147A-f	5′-GTACGTTTGCTGGCGGCGAGCGGCGGCAAGTC-3′
K147A-r	5′-GACTTGCCGCCGCTCGCCGCCAGCAAACGTAC-3′